Mechanism and kinetics of excitedstate relaxation in internally hydrogenbonded molecules: 2(2′hydroxy5′methylphenyl)benzotriazole in solution

Alan L. Huston, Gary W. Scott, and Amitava Gupta

Citation: The Journal of Chemical Physics **76**, 4978 (1982); doi: 10.1063/1.442844
View online: http://dx.doi.org/10.1063/1.442844
View Table of Contents: http://scitation.aip.org/content/aip/journal/jcp/76/10?ver=pdfcov
Published by the AIP Publishing

Mechanism and kinetics of excited-state relaxation in internally hydrogen-bonded molecules: 2-(2′-hydroxy-5′-methylphenyl)-benzotriazole in solution[a)]

Alan L. Huston and Gary W. Scott

Department of Chemistry, University of California, Riverside, Riverside, California 92521

Amitava Gupta

Energy and Materials Research Section, Jet Propulsion Laboratory, California Institute of Technology, Pasadena, California 91103

(Received 9 July 1981; accepted 9 February 1982)

We report the ground state absorption recovery kinetics (at 355 nm) and the fluorescence spectra and kinetics of 2-(2′-hydroxy-5′-methylphenyl)-benzotriazole (I) following excitation at 355 nm in several solvents at room temperature. Measured lifetimes range from 14 to 75 ps. Fluorescence lifetimes are shorter than the corresponding ground state recovery times, indicating the intervention of intermediate forms during the excited state relaxation process. The measured fluorescence quantum yield is lower than one predicted by the usual calculated radiative rate for the near UV, strongly absorbing singlet state of this molecule. Decay rates are slower in ethanol than in nonhydrogen bonding solvents indicating that external interference with the intramolecular hydrogen bond in (I) slows the relaxation rate. The room temperature decay rates are not strongly affected by the solvent viscosity. Deuteration of the molecule produces only a slightly more rapid ground state recovery rate than in the protonated species. A model involving excited state proton transfer is presented for the decay mechanism, rationalizing the known experimental data.

I. INTRODUCTION

Intramolecular hydrogen bonds, present in a number of molecules containing phenolic hydroxyl groups and slightly basic carbonyl or amino groups, lead to a variety of interesting and unusual photophysical and photochemical properties.[1–21] Many of these molecules, such as derivatives of 2-hydroxybenzophenone and 2-(2′-hydroxyphenyl)-benzotriazole, are widely used as ultraviolet - absorbing polymer photostabilizers.[22,23] The intramolecular hydrogen bond in these molecules is thought to promote rapid, radiationless, excited-state decay. Large Stokes shifts observed in the emission spectra of many of these molecules suggest that excited-state proton transfer plays an important role in the excited-state relaxation mechanism. The mechanism and kinetics of these processes have yet, in many cases, to be determined. Related kinetics studies include work on salicylates,[7–9] salicylanilides,[10] 2-(2′-hydroxyphenyl-s-triazines,[6] 2-hydroxybenzophenones,[11–16] and 2-(2′-hydroxyphenyl)-benzotriazoles.[14,15,19]

In the present paper, we present new kinetic and spectroscopic studies of the mechanism of excited-state decay for 2-(2′-hydroxy-5′-methylphenyl)-benzotriazole (I) in room temperature solution. The ground-state structure of (I) in aprotic solvents and one possible tautomeric form (I′) resulting from ultraviolet excitation of (I) are shown in Fig. 1. Also shown in Fig. 1 is a possible ground state structure (II) for this molecule in an alcoholic solvent. The intermolecular hydrogen bonds illustrated by structure (II) could prevent or partially interfere with the formation of the intramolecular hydrogen bond which promotes the process (I) → (I′). The present investigation explores the mechanism and kinetics of the processes of ultraviolet excitation and excited state decay (I) ⇄ (I′) as well as the importance of structures like (II) in protic solvents. These studies include measurements of ground-state absorption bleaching and recovery kinetics, as well as excited-state fluorescence kinetics of (I) in both protic and aprotic solvents at room temperature. Also, determinations of room temperature fluorescence spectra and quantum yields are reported. An analysis of the results produced by these techniques gives rates of ex-

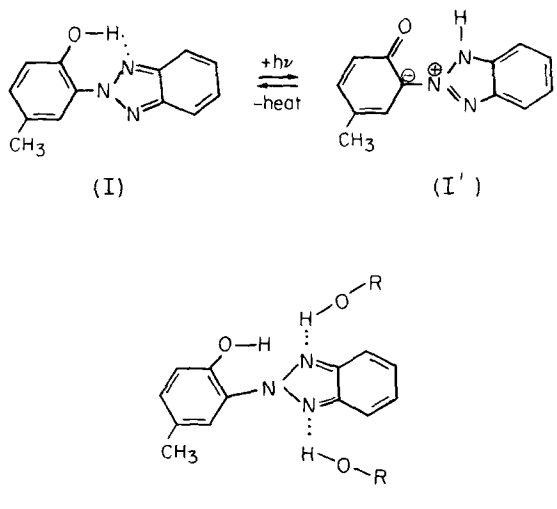

FIG. 1. Ground-state (I) and excited-state (I′) molecular structures of 2-(2′-hydroxy-5′-methylphenyl)-benzotriazole in aprotic solvents. Also shown is a possible structure (II) in alcoholic solvent.

[a)]This research was supported by the Polymer RAD task of the Solar Thermal Power Systems Project of the Jet Propulsion Laboratory, the University of California Appropriate Technology Program, and the Committee on Research at the University of California, Riverside.

 0021-9606/82/104978-08$02.10

cited-state relaxation processes, as well as a mechanism of the excited-state decay in this molecule.

II. EXPERIMENTAL TECHNIQUES

A. Samples

Commercially available 2-(2′-hydroxy-5′-methylphenyl)-benzotriazole (Tinuvin P, Ciba-Geigy) was purified by zone refining for 100 zone passes. Some of the solvents used Ethanol (200 proof, Pharmco), Methylene Chloride (SpectrAR, Mallinckrodt), and Methylcyclohexane (Omni Solv glass distilled, MCB), were dried over molecular sieve. In addition, cyclohexane was dried over Lithium Aluminum Hydride and distilled under vacuum prior to use. (These precautions were taken to assure that trace amounts of water would not have an effect on the measured kinetics or spectra.) Solutions were prepared to have a ground-state optical density at 355 nm of ≈ 1.0 in a 1 mm path quartz cell for the ground-state absorption bleaching experiments and of > 2 in 1 mm for the fluorescence experiments. [These ground-state optical densities were chosen to optimize the signal/noise ratio (bleaching experiment) or to minimize detrimental geometrical effects on the time resolution (fluorescence experiments)].

The monodeutero-substituted derivative of (I) was prepared by shaking a solution of (I) in methylcyclohexane with D_2O. Essentially complete exchange of the phenolic hydrogen for deuterium in (I) was confirmed by proton NMR, both before and after the kinetics measurements were made. (This sample was handled in a helium-filled glove bag to prevent contamination by atmospheric H_2O.)

B. Ground-state absorption bleaching recovery kinetics

Absorption recovery kinetics were obtained using a single third-harmonic pulse ($\Delta t \approx 10$ ps, $\lambda = 355$ nm) from a modelocked Nd^{3+}: silicate glass laser system. Approximately 90% of the focused UV pulse (excitation pulse) was used to bleach the ground-state absorption of the sample. This pulse, containing ~0.3 mJ, was focused on an ~700 μm diameter aperture at the sample. The remainder of the UV pulse (probe pulse) followed a variable delay line and was used to monitor changes in the sample absorption as a function of time following excitation. The angle between the pump and probe pulse paths was ~6°. The probe pulse absorption by the sample was determined by comparing the intensity of a small portion of the probe pulse, split off prior to passing through the sample, with its intensity after passing through the sample. Pulses were detected on a fast biplanar photodiode with a Tektronix 7904 oscilloscope. Exponential decay curves were fit to the experimental data, after convolution with the excitation and probe pulse widths.

C. Excited-state fluorescence kinetics

The fluorescence kinetics of (I) in several solvents were performed using the streak camera facility of the Regional Laser Laboratory at the University of Pennsylvania. Front surface excitation of the sample was accomplished with the third harmonic of a TEM_{00} modelocked Nd^{3+}: silicate glass laser system. Sample fluorescence, isolated with suitable bandpass filters, was imaged on an ~600 μm pinhole which was in turn imaged on the photocathode of a GEAR Pico V streak camera, used at its maximum streak speed. The streaked fluorescence image was detected and digitized with an ISIT vidicon of an optical multichannel analyzer (PARC, OMA 2). Streak speed and intensity calibration were simultaneously accomplished with a suitably attenuated, second-harmonic pulse which passed through a fixed-separation etalon ($l = 6.23$ mm). The second-harmonic pulse was diffused and directed to an identical pinhole, whose image was streaked at the same time as the fluorescent image. Using the apparatus in this configuration, an attenuated excitation pulse, scattered from a scattering plate at the sample cell position, had an apparent width of 15 ps. (The actual laser pulse width was ~7 ps, but the streak camera was not used at its maximum time resolution of 2 ps, in order to increase its experimental sensitivity.)

For each sample, at least five separate determinations of fluorescence streaks were obtained. However, only those streaks from clean, single excitation pulses that were suitably "framed" by the streak were considered in the data analysis (i.e., the laser pulse was captured by the camera streak after the first quarter and before the first half of the streak). In some of the experiments (ethanol solvent) the fluorescence intensities were strong enough so that the streaks could be analyzed individually. In other experiments, several streaks were averaged together before data analysis.

For each experiment, the data were analyzed in the following way: (1) The time base calibration was obtained (for individual streaks) by using the simultaneously obtained streaks of etalon-generated peaks to calibrate the channel number in time using an OMA "built-in" cubic function fit. Usually five or six etalon peaks (separated by 41.6 ps) were used in this calibration. (2) For the experiments in which the data were averaged before analysis (methylene chloride and methylcyclohexane solvents), the individual fluorescence streaks that were to be averaged were shifted (in channel number) so that the first etalon peak for each was superimposed at the same channel number. They were then summed in the OMA and an average time calibration determined from the individual etalon traces. (In general, the variation in etalon peak separation from peak-to-peak and from shot-to-shot was less than ~3%.) (3) The intensity vs time data thus obtained were transferred in digital form from the OMA 2 console to a Hewlett–Packard 85 minicomputer for final data analysis. Also obtained and transferred in a similar way was an experiment of intensity vs time data for a typical, scattered 355 nm laser pulse. (4) Using the H–P 85 computer, experimental fluorescence lifetimes were obtained by deconvolution of the fluorescence kinetics experiments from the detector response to the scattered laser pulse experiment with simultaneous least-squares fitting to an (assumed) exponential decay.[24–27] The data were therefore, least-

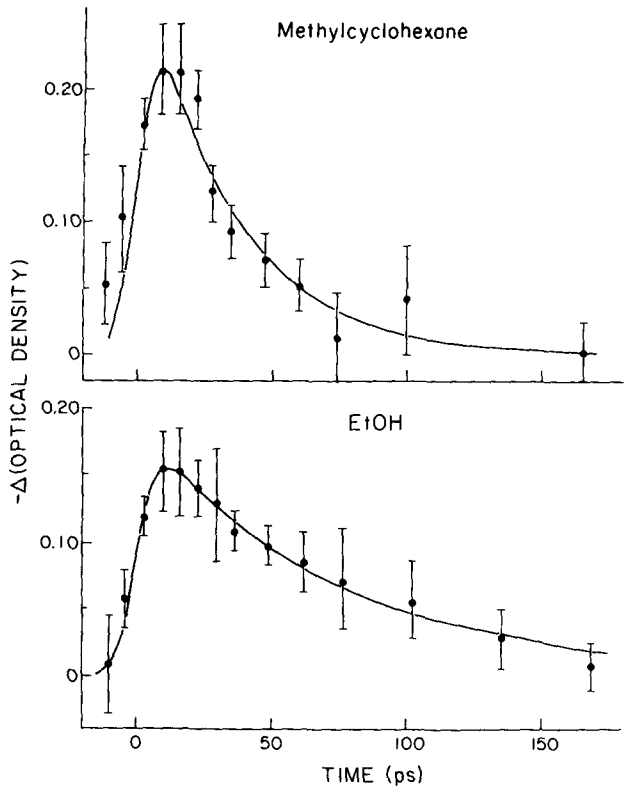

FIG. 2. Transient optical density changes (decreases), due to (I) at 355 nm following excitation at the same wavelength. The sample, in a 1 m cell, had an optical density at 355 nm under low light level conditions of ~1.0. The ♣ are the average of the experimental optical density changes. The smooth curves are exponential decaying functions, best fit to the data, after convolution to account for the finite duration of the laser excitation and probe pulses. (a) Methylcyclohexane solvent, (b) ethanol solvent.

squares fit with the following function:

$$C(t) = Ae^{-t/\tau} \int_0^t S(t')\, e^{t'/\tau} dt' + B, \qquad (1)$$

in which

$C(t)$ are the fluorescence intensities as a function of time,

$S(t)$ are the scattered pulse intensities as a function of time,

and A, B, and τ (the lifetime) are adjustable parameters.

(5) Since there was some uncertainty in the position of $t = 0$ (the time position corresponding to the peak of the excitation pulse) in the fluorescence kinetics experiments, the relative time between the fluorescence kinetics experiments and the scattered laser pulse experiment were varied over a range of ~5 ps during the fitting process. The minimum root-mean-square (rms) value determined for each experiment in this range was taken to be the best fit to the data, and the lifetime (τ) determined in this best fit is reported below in Sec. III.

D. Fluorescence spectra and quantum yields

Room temperature emission spectra and quantum yields of (I) in ethanol, methylene chloride, methylcyclohexane, and cyclohexane were obtained under steady-state illumination conditions. Both a Perkin-Elmer MPF3A spectrofluorimeter, fitted with an automatic spectral correction accessory, and another high sensitivity spectrofluorimeter[28] were used in the determinations of fluorescence spectra and quantum yields. In addition, the room temperature emission spectra of (I) in methylcyclohexane and in ethanol were obtained using a conventional laser Raman spectrometer equipped with an argon ion laser Raman spectrometer equipped 363 nm), $f/1.0$ UV collection optics, a 0.85 m double monochromator (Spex 14018), and a cooled photomultiplier (Hamamatsu R955) used in the photon counting mode.

III. EXPERIMENTAL RESULTS

Representative absorption recovery kinetics data at 355 nm for (I) in methylcyclohexane and in ethanol are shown in Figs. 2(a) and 2(b), respectively. Absorption recovery kinetics of (I)d_1 in methylcyclohexane are shown in Fig. 3. The experimental recovery lifetimes, determined in the least-squares fit, are given in the summary in Table I. In all cases, the absorption recovery was complete at the longer delay times investigated with the change in optical density at 355 nm returning to zero within experimental error. No evidence for nonexponential decay behavior was observed in these experiments, again within experimental error.

The fluorescence decay kinetics of (I) in ethanol (fluorescence excited by a single laser shot), methylcyclohexane (fluorescence average due to four laser shots), and methylene chloride (fluorescence average due to three laser shots) are shown in Figs. 4(A), 4(B), and 4(C), respectively. In Fig. 5, the fluorescence intensity vs time data for (I) in ethanol, averaged for five laser shots, are plotted on a semilogarithmic scale, together with the best fit in a least-squares sense of an exponential decay to this data. (Only fluorescence intensity data starting ~25 ps after the peak of the fluorescence intensity are reproduced in this figure.)

The streak-camera-detected fluorescence of (I) in methylcyclohexane and in methylene chloride solvents was somewhat weaker than it was in ethanol solvent.

TABLE I. Summary of room temperature excited-state kinetics in 2-(2′-hydroxy-5′-methylphenyl)-benzotriazole.

Solvent	Absorption recovery τ (ps) at 355 nm	Fluorescence decay τ (ps)
Methylcyclohexane:		
(I)	33 ± 5	14.4 ± 3.4
(I)-d_1	22 ± 5	•••
Ethanol	74 ± 10	52.0 ± 3.8
Methylene chloride	29 ± 5	19.1 ± 4.8
Hexadecane	33 ± 3	•••

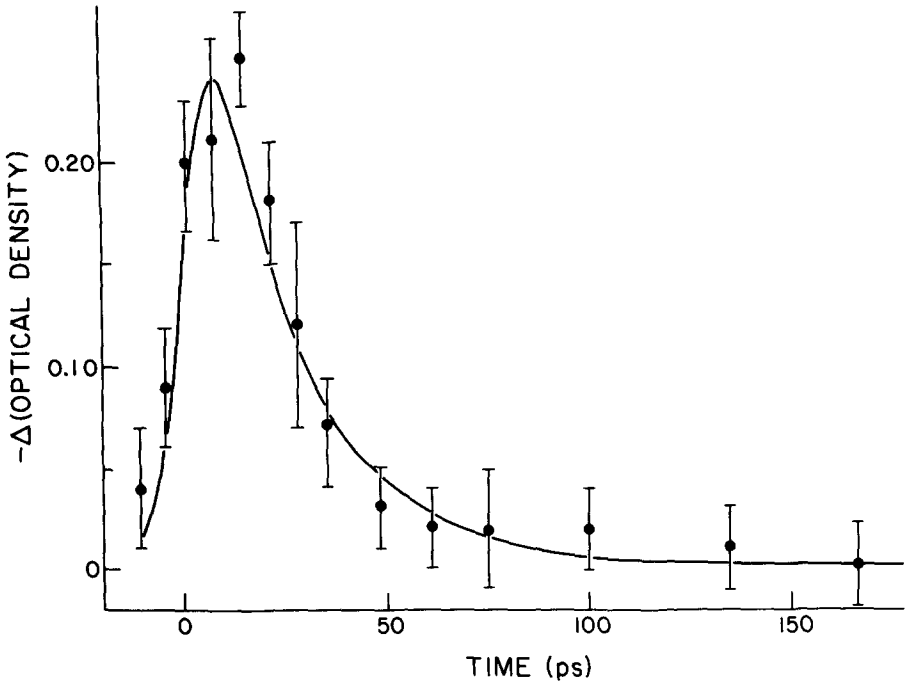

FIG. 3. Transient optical density changes (decreases) of (I)-d_1 in methylcyclohexane at 355 nm. Other conditions were the same as those indicated in the caption of Fig. 1.

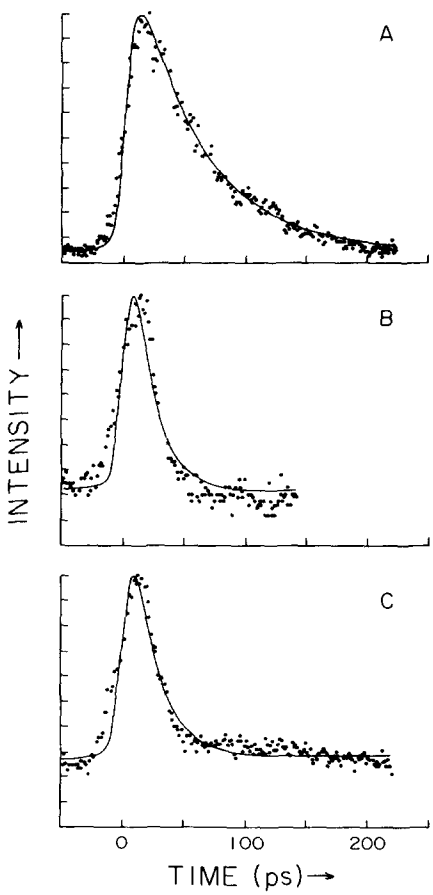

FIG. 4. Streak camera record of the fluorescence intensity ($\lambda \gtrsim 400$ nm) vs time of (I) after excitation at 355 nm; (a) ethanol solvent (single laser shot record), (b) methylcyclohexane solvent (average of four laser shot records), (c) methylene chloride solvent (average of three laser shot records).

This is principally a result of the reduced lifetimes observed in the former solvents.

The values of the fluorescence lifetimes and estimated errors in these lifetimes are given in Table I. These values were obtained as follows: For (I) in ethanol, the value of the lifetime was obtained, as described in Sec. IIC from a least-squares fit to the individual fluorescence decay data for five different laser shots. [One of these five decay data sets is shown in Fig. 4(A).] These values ranged from 48.7 to 58.4 ps. The average value (52.0 ps) and the standard deviation in this average (3.8 ps) are the numbers reported in Table I. For (I) in methylcyclohexane and in methylene chloride, only a single set of averaged decay data were subjected to the least-squares fitting process. [These

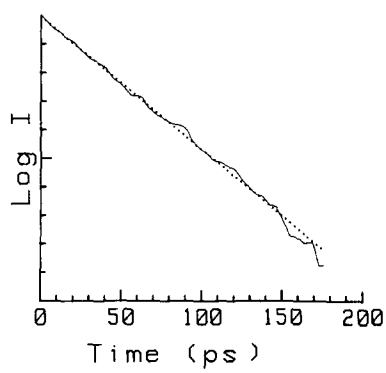

FIG. 5. Semilogarithmic presentation of the fluorescence decay of (I) in ethanol after averaging five laser shot records of the type shown in Fig. 4(a). The dotted curve is a least-squares fit exponential decay ($\tau = 53$ ps) to the experimental data (solid curve). The ordinate scale ranges from 0 to 4.

data sets are shown in Figs. 4(B) and 4(C), respectively.] The lifetime values obtained in these two fits are reported in Table I. The error estimates for these values were obtained by assuming the uncertainty in the position of $t=0$ was ±4 channels (see Sec. IIC) of the OMA (~±2.5 ps), thereby obtaining the range of lifetimes reflected by the error estimates given in Table I. These error estimates were always larger (by ~5×) than the standard deviation in the lifetime parameter obtained in the minimum rms (best) fit. (This same procedure was also applied to each single-laser-shot-produced, ethanol solvent data set, and resulted in error estimates, which were approximately the same as the standard deviation in the average reported in Table I. It should be noted that the "best" fits obtained for each single-laser-shot data set established the position of $t=0$ relative to the etalon marker pulse to within ±2 channels from data set to data set.)

In Fig. 4 and for the fluorescent lifetimes given in Table I, the only wavelength discrimination of the fluorescence was provided by a UV blocking filter (Schott, GG 400) to isolate the fluorescence from the laser pulse. For (I) in ethanol only, the short-lived emission was strong enough to allow the use of narrower bandwidth filters to determine the wavelength range of the fluorescence. For example, allowing only emission wavelengths in the range 400 nm $\lesssim\lambda\lesssim$ 460 nm (Schott GG 400×3 mm, Schott BG 14×3 mm, and Ditric 4600 short-pass cut-off filters), essentially identical emission kinetics were observed for (I) in ethanol as those given in Fig. 4 and Table I. (The best-fit lifetimes for averaged data from three laser shots was in this case 50.1 ps with an error estimate of ±7.8 ps.) On the other hand, for the same sample, blocking all emission wavelengths shorter than ~570 nm (Schott OG 570×3 mm) resulted in a streaked fluorescence signal only barely discernible above background; i.e., less than a few percent of the total short-lived detected visible fluorescence was in a wavelength region to the red of 570 nm. Steady-state emission spectra indicate that fluorescence maxima of (I) in all solvents at room temperature occurs at $\lambda_{max}\lesssim 410$ nm. (See below.)

The short-lived fluorescence kinetics of (I) in ethanol were found to follow an exponential decay, within experimental error, as shown in Fig. 5. The short-lived fluorescence kinetics in methylcyclohexane and methylene chloride were too weak to allow for exact determination of the form of the decay, but were assumed to also be exponential in the fitting procedure.

Broad, featureless emission spectra were observed for (I) in methylene chloride, ethanol, methylcyclohexane, and cyclohexane solvents at room temperature. Initial experiments with the commercial spectrofluorimeter on (I) in the methylene chloride and ethanol solvents indicated very weak emission with maxima in the blue and fluorescence quantum yields on the order of $\sim 2\times10^{-5}$. Subsequently, quantum yield estimates were made using the high sensitivity spectrofluorimeter[28] on (I) in cyclohexane. In this case the emission maximum was at $\lambda_{max}\sim 410$ nm, and the fluorescence quantum yield was estimated to be in the range 2×10^{-5} to 5×10^{-5}. Finally, emission spectra of (I) were obtained with the laser Raman spectrometer (see Sec. IID) in the solvents cyclohexane, methylcyclohexane and ethanol. In every case, the emission maximum occurred in the range $\lambda_{max}\sim 405$–410 nm and the emission intensities were similar. No emission intensity was observed to the red of ~500 nm.

IV. DISCUSSION

A. Excited-state kinetics

The kinetics data presented above provide new information concerning the excited-state decay mechanism of (I). In the first place, in three solvents, the fluorescence decay of (I) was found to occur faster than did the ground-state absorption recovery of (I) at 355 nm. This observation suggests a mechanism involving sequential decay of the fluorescent state through other intermediate state(s) and/or tautomeric form(s) before ground-state recovery is complete. This model might require that the ground-state recovery be somewhat nonexponential but deviations from nonexponential behavior need not be too severe and could easily be masked by the signal-to-noise evidenced by the experimental data (Figs. 2 and 3). From the present ground-state absorption recovery experiments on (I), it is clear that no significant quantum yield of long-lived species is obtained. These results indicate that the major decay pathway involves only singlet species of the molecule.

Another important feature of our results is that both the fluorescence decay and the ground-state absorption recovery lifetimes of (I) are longer in the intermolecular hydrogen bonding solvent (ethanol) than in the non-hydrogen bonding solvents. This observation suggests that the ethanol solvent may competitively form *intermolecular* hydrogen bonds with (I), disrupting the intramolecular hydrogen bond and slowing the excited-state relaxation process as suggested in Sec. I and in Fig. 1.

To investigate the possibility that the kinetics of radiationless deactivation of (I) is affected by solvent viscosity, the ground-state recovery kinetics of (I) was investigated in two different hydrocarbon solvents of different viscosity at room temperature: methylcyclohexane ($\eta=0.73$ cp) and hexadecane ($\eta=3.34$ cp). Viscosity-dependent nonradiative rate constants have been determined previously for a number of molecules containing internally rotating phenyl groups.[29–33] If *free* rotation about the C–N single bond joining the phenol and benzotriazole parts of (I) modified its radiationless decay rate in the same way[33] then the decay time observed in hexadecane would be expected to be ~50% longer than in methylcyclohexane. The lack of a viscosity effect on the nonradiative decay rate in (I) suggests that rotation about the C–N bond may be hindered, most likely due to the intramolecular hydrogen bond. In the case of a hindered rotor, it is not clear that the macroscopic viscosity of the solvent is the correct parameter to use in describing the microenvironment of the solute. However, emission studies, discussed below, indicate that the dihedral angle between the phenol

and benzotriazole planes plays a significant role in the decay mechanism.

The effect of deuteration of the hydroxyl group on the rate of relaxation of (I) was investigated using the ground state recovery technique. The measured rate in the deuterated form of (I) was somewhat faster than for the protonated form, although the rates are nearly within experimental error of each other. The fact that a *normal* deuterium isotope effect was not observed indicates that the decay mechanism is not controlled by activated proton transfer or proton tunneling.

B. Emission spectra and quantum yields

A small Stokes shift was obtained for room temperature emission spectra of (I) with λ_{max} ~410 nm in all solvents. The state or species responsible for this emission is not the same one that is responsible for the low temperature, solid phase emission of (I) previously reported in an aprotic matrix[17,18] and confirmed by us (λ_{max} ~600 nm).[34] Whereas, this red emission of (I) in the solid phase is presumably due to a proton-transferred tautomeric form of the molecule, the 410 nm emission in room temperature liquids is probably due to a nonproton-transferred form of the molecule.

The low emission quantum yields observed for (I) in room temperature liquids, however, are not consistent with a purely vertical excited state, one in which the molecular conformation is the same as the ground state's. For example, the radiative lifetime of the vertically excited state of (I) can be obtained, in the conventional picture,[35] by integrating the low energy band(s) of the absorption spectrum. The radiative lifetime, thus determined, turns out to be ~10 or ~4 ns, depending upon whether only the lowest or the two lowest energy bands are included in the integration. This then predicts, for fluorescent lifetimes in the range 14 to 52 ps, that the fluorescence quantum yields should be in the range 10^{-2} to 10^{-3}, or 20 to 500 times larger than actual measured fluorescence quantum yields. Therefore, nonvertical forms of the molecule must be rapidly available from the initially excited form. These forms most likely involve either nonplanar conformations of the molecule or highly excited O–H stretch vibrational states of the molecule as discussed in Sec. IV C below. These forms are probably responsible for the observed room temperature fluorescence of this molecule in liquids.

C. A consistent model for excited-state relaxation

Several groups[4,17–19] have presented a mechanistic model for the singlet decay of (I) which, with slight modification of details, can be shown to be consistent with the known experimental results. The steps in this model are as follows:

$$\begin{aligned} &\text{(a) UV Excitation: } S_0 \rightarrow S_1, \\ &\text{(b) Proton transfer tautomerization: } S_1 \rightarrow S_1', \\ &\text{(c) Internal conversion: } S_1' \rightarrow S_0', \\ &\text{(d) Proton back transfer: } S_0' \rightarrow S_0. \end{aligned} \tag{2}$$

In this model, S_0 is the ground state of (I); S_1 the initially excited singlet state of (I); S_1' an excited singlet state of a proton-transferred tautomer [e.g., (I′) of Fig. 1]; and S_0' the corresponding ground state of (I′).

Assuming this mechanism is correct, then the room temperature blue fluorescence we report above would be assigned to $S_1 \rightarrow S_0$ emission, it being only moderately Stokes shifted from the absorption. In fluid solution only this blue fluorescence of (I) is observed. However, when (I) in cyclohexane or methylcyclohexane is cooled somewhat below the melting point of these solvents (~260 and ~200 K, respectively), red emission from (I) has been observed[34] as mentioned in Sec. IV B. This emission, previously observed at 90 K and assigned to $S_1' \rightarrow S_0'$,[17,18] is not observed in fluid solution. The discrepancy between the measured and calculated fluorescence quantum yields of the blue fluorescence may seem inconsistent with these assignments, however, the model will accommodate these experimental facts as shown below.

While the above data may seem inconsistent, there is in fact a consistent model which neatly rationalizes the experimental observations. The key feature of this model is that the initially excited state of the molecule (S_1) may be in equilibrium with the proton transferred form (S_1') on the picosecond time scale, perhaps by virtue of slow vibrational relaxation in comparison with rapid proton transfer. Therefore, the observed emission is from vibrationally hot molecules of (I) with actual fluorescence quantum yields significantly diminished by dilution with "hot" molecules of the form (I′). (See Fig. 1.) The fluorescence decay time then reflects internal conversion of this (I′) form, which is in equilibrium with the (I) form. Hence, step (2b) above should be written as an equilibrium and step (2c) occurs before vibrational relaxation. The lack of any observable red emission in room temperature fluid solution probably reflects the decreased quantum yield for this process, due to more rapid internal conversion prior to vibrational relaxation. Further, emission of the form $(S_1')^* \rightarrow (S_0')^*$ might in this model be red-shifted from $S_1' \rightarrow S_0'$ emission, but it has not yet been observed.

It should be noted that there is evidence in the literature that vibrational relaxation times of large molecules in room temperature solution can be as long as 10–20 ps or so. For example, stilbene in room temperature solution exhibits an excited-state vibrational relaxation time of ~25 ps[36] while in dibenzpyrene, this time has been estimated as ~15 ps.[37] Whether excited-state vibrational relaxation times of (I) in room temperature solution can be slower than ~15 ps is still an open question, but the spectroscopic evidence cited above tends to confirm that they can be. (In ethanol, slowing of the equilibration process by competing intermolecular hydrogen bonding extends the fluorescence decay and the model does not really require that vibrational relaxation in ethanol be as slow as 50 ps, only that the equilibrium process be rate determining.)

Other experimental results are readily accommodated

by this model. The fluorescence decay times are shorter than the ground-state recovery times because most molecules evolve into proton-transferred ground-state forms of (I'), i.e., S_0'. Ground-state recovery times then include the additional time for step (2d) of back proton transfer so that both internal conversion and back transfer contribute to the observed rate. The observation that fluorescence decay times are slowed in ethanol probably reflects the slowing of establishment of equilibrium in step (2b), due to the interferring nature of the intermolecular hydrogen bonds formed by the solvent with (I). Internal conversion rates would also be expected to change, since the solvent modifies the excited-state potential surface.

The viscosity effect is not quite so clear cut. Internal phenol rotation in this molecule is, at best, hindered and the microscopic viscosity dependence of this motion may be weaker than in molecules which undergo free internal rotation. Thus, it might be argued that step (2c) is promoted by relative librational motion of the phenol and benzotriazole portions of the molecule. Evidence concerning the importance of this librational motion on the rate of internal conversion manifests itself in the observation of relaxed red fluorescence in aprotic rigid matrices in which the amplitude of the relative motion would be less than in fluid solution. In any case, the ground-state recovery times measured in hexadecane and methylcyclohexane give the rates of composite processes, and hence may not be very sensitive to the modest viscosity difference in these two solvents.

The deuteration effect on ground-state recovery times eliminates rate-determining proton tunneling or activated proton transfer from the excited-state relaxation model. In the proposed model, it is not clear what the effect of deuteration of the molecule should have on the rate of the overall process of internal conversion and back proton transfer [steps (2c) and (2d)]. For example, the rates of internal conversion processes depend on the density of vibronic states and Franck–Condon factors of the lower energy state to which decay occurs. These factors could conceivably be affected by deuteration in such a way that the radiationless process would be more rapid in the deutero derivative than in the proto, so the model is consistent with the experimental observations.

Other workers have reported kinetic solvent effects on the relaxation of similar molecules. For example, a similar solvent effect was observed on ground state recovery kinetics reported for 2-hydroxybenzophenone.[11] In that molecule, complete ground-state recovery was determined to occur exponentially with a lifetime of 35 ± 5 ps in hexane solvent. In ethanol, however, the ground-state absorption recovery proceeded in a nonexponential fashion: a fast component of ~30 ps and a slow component of 1.5 ns.[11] For that molecule, the authors proposed the presence of two different ground-state species in ethanol (e.g., an intramolecular hydrogen-bonded molecule and a molecule intermolecularly hydrogen-bonded to the solvent) as a possible explanation of the results. The long time component of the ground-state recovery was assigned to a triplet decay route, tentatively attributed to those molecules hydrogenbonded to the solvent. In the present ground-state absorption recovery experiments on (I), however, no long-lived species were observed, either in ethanol or the other solvents. Furthermore, although the possibility of more than one ground-state species cannot be ruled out for (I) in ethanol, there is no evidence in either the fluorescence or the ground-state recovery kinetics for nonexponential decay. Therefore, there is no reason to invoke more than one ground-state form of (I) in ethanol.

Recently, Smith and Kaufmann[9] presented a model which considers the effect of the dielectric strengths of the solvent on the nonradiative decay rate of the related molecule methyl salicylate. In contrast to the present results, they observe *shorter* fluorescence lifetimes in hydrogen-bonding solvents than in hydrocarbons. They attribute this to an increased intersystem crossing rate in these solvents caused by a decreased singlet–triplet energy gap in the zwitterionic form of the molecule. In the case of (I), there is no experimental evidence that intersystem crossing is a significant radiationless decay route in room temperature fluid solution, nor is any highly Stokes shifted (zwitterionic) emission of (I) observed under these conditions.

In conclusion, the kinetic and spectroscopic data presented above provide new information concerning the excited-state decay mechanism of (I). The model of this decay mechanism is as follows:

$$\begin{aligned}
&\text{(a) UV excitation: } S_0 \rightarrow S_1^*, \\
&\text{(b) Proton transfer tautomerization: } S_1^* \rightleftarrows (S_1')^*, \\
&\text{(c) Internal conversion: } (S_1')^* \rightarrow (S_0')^*, \text{ and} \\
&\text{(d) Vibrational relaxation and proton back transfer: } (S_0')^* \rightarrow S_0 ,
\end{aligned} \tag{3}$$

in which "'" indicates a proton-transferred form and "*" a vibrationally unrelaxed state. Fluorescence of (I), observed in room temperature fluid solution with a normal Stokes shift, is attributed to a vibrationally unrelaxed excited state S_1^*, which is in equilibrium with the proton-transferred excited state $(S_1')^*$ of the molecule. Internal conversion $(S_1')^* \rightarrow (S_0')^*$ controls the lifetime of this fluorescence, while ground-state recovery rates include additional contributions from vibrational relaxation and proton back transfer in the ground state.

ACKNOWLEDGMENTS

We wish to thank Professor Robin Hochstrasser, Director of the Regional Laser Laboratory at the University of Pennsylvania, for providing to us the opportunity to conduct the streak camera measurements of fluorescence decay in that laboratory. We appreciate the expert guidance and assistance of Mr. Dan Negus during the course of these experiments at the Regional Laser Laboratory. One of us (GWS) wishes to thank Professor Bryan Kohler for helpful discussions regarding this work and for his warm hospitality

at Wesleyan University. We also thank Ms. Linda DeLucci for preparation of the manuscript.

[1]J. R. Merrill and R. G. Bennett, J. Chem. Phys. **43**, 1410 (1965).
[2]A. A. Lamola and L. J. Sharp, J. Phys. Chem. **70**, 2634 (1966).
[3]J. P. Guillory and C. F. Cook, J. Am. Chem. Soc. **95**, 4885 (1973).
[4]J. A. Otterstedt, J. Chem. Phys. **58**, 5716 (1973).
[5]W. Klöpffer, Adv. Photochem. **10**, 311 (1977).
[6]H. Shizuka, K. Matsui, Y. Hirata, and I. Tanaka, J. Phys. Chem. **80**, 2070 (1976); **81**, 2243 (1977).
[7]K. K. Smith and K. J. Kaufmann, J. Phys. Chem. **82**, 2286 (1978); and in *Laser Chemistry*, edited by A. H. Zewail (Springer, Berlin, 1978), p. 163.
[8]D. Ford, P. J. Thistlethwaite, and G. J. Woolfe, Chem. Phys. Lett. **69**, 246 (1980).
[9]K. K. Smith and K. J. Kaufmann, J. Phys. Chem. **85**, 2845 (1981).
[10]P. J. Thistlethwaite and G. J. Woolfe, Chem. Phys. Lett. **63**, 401 (1979).
[11]S.-Y. Hou, W. M. Hetherington III, G. M. Korenowski, and K. B. Eisenthal, Chem. Phys. Lett. **68**, 282 (1979).
[12]C. Merritt, G. W. Scott, A. Gupta, and A. Yavrouian, Chem. Phys. Lett. **69**, 169 (1980).
[13]A. Gupta, A. Yavrouian, S. DiStefano, C. D. Merritt, and G. W. Scott, Macromolecules **13**, 821 (1980).
[14]A. Gupta, G. W. Scott, and D. Kliger, ACS Symposium Series 151 (ACS, Washington, 1980), Chap. 3.
[15]A. L. Huston, C. D. Merritt, G. W. Scott, and A. Gupta, in *Picosecond Phenomena II*, edited by R. M. Hochstrasser, W. Kaiser, and C. V. Shank (Springer, Berlin, 1980), p. 232.
[16]K. J. Choi, L. A. Halliday, and M. R. Topp, in Ref. 15, p. 131.
[17]T. Werner, J. Phys. Chem. **83**, 320 (1979).
[18]T. Werner, G. Wössner, and H. E. A. Kramer, ACS Symposium Series 151 (ACS, Washington, 1980), Chap. 1.
[19]T. Werner and H. E. A. Kramer, Europ. Polym. J. **13**, 501 (1977).
[20]A. U. Acuña, F. Amat-Guerri, J. Catalán, and F. González-Tablas, J. Phys. Chem. **84**, 629 (1980), and references therein.
[21]L. A. Heimbrook, J. E. Kenny, B. E. Kohler, and G. W. Scott, J. Chem. Phys. **75**, 5201 (1981).
[22]H. J. Heller, Europ. Polym. J. Suppl. **105**, 105 (1969).
[23]B. Ranby and J. F. Rabek, *Photodegratation, Photooxidation, and Photostabilization of Polymers: Principles and Applications* (Wiley, New York, 1975).
[24]S. S. Brody, Rev. Sci. Instrum. **28**, 1021 (1957).
[25]A. Hang, B. E. Kohler, E. B. Priestly, and G. W. Robinson, Rev. Sci. Instrum. **40**, 1439 (1969).
[26]J. N. Demas and G. A. Crosby, Anal. Chem. **42**, 1010 (1970).
[27]W. R. Ware, in *Creation and Detection of the Excited State* 1*A*, edited by A. A. Lamola (Marcel Dekker, New York, 1971), Chap. 5.
[28]S. F. Rice and H. B. Gray (unpublished results).
[29]C. V. Shank, E. P. Ippen, O. Teshke, and K. B. Eisenthal, J. Chem. Phys. **67**, 5547 (1978).
[30]Th. Förster and G. Hoffman, Z. Phys. Chem. (Leipzig) **75**, 63 (1971).
[31]D. Magde and M. W. Windsor, Chem. Phys. Lett. **24**, 144 (1974).
[32]E. P. Ippen, C. V. Shank, and A. Bergman, Chem. Phys. Lett. **38**, 611 (1976).
[33]W. Sibbett, J. R. Taylor, and D. Welford, IEEE J. Quantum Electron. **17**, 500 (1981).
[34]A. L. Huston and G. W. Scott (unpublished results).
[35]S. J. Strickler and R. A. Berg, J. Chem. Phys. **37**, 814 (1962).
[36]B. I. Greene, R. M. Hochstrasser, and R. B. Weisman, Chem. Phys. Lett. **62**, 427 (1979).
[37]K.-J. Choi and M. R. Topp, Chem. Phys. Lett. **69**, 441 (1980).